Published in final edited form as:
Neuron. 2010 February 25; 65(4): 503–515. doi:10.1016/j.neuron.2010.01.035.

The immune protein CD3ζ is required for normal development of neural circuits in the retina

Hong-ping Xu[1], **Hui Chen**[2], **Qian Ding**[3], **Zheng-Hua Xie**[3], **Ling Chen**[2], **Ling Diao**[4], **Ping Wang**[2], **Lin Gan**[3], **Michael C. Crair**[1], and **Ning Tian**[2,*]

[1]Department of Neurobiology, Yale University School of Medicine, New Haven, CT 06520, USA

[2]Department of Ophthalmology and Visual Science, University of Utah School of Medicine, Salt Lake City, UT 84132, USA

[3]Department of Ophthalmology, University of Rochester, Rochester, NY 14642, USA

[4]Department of Biology, Yale University, New Haven, CT 06520, USA

Summary

Emerging evidence suggests immune proteins regulate activity-dependent synapse formation in the central nervous system (CNS). Mice with mutations in class I major histocompatibility complex (MHCI) genes have incomplete eye-specific segregation of retinal ganglion cell (RGC) axon projections to the CNS. This effect has been attributed to causes that are non-retinal in origin. We show that a key component of MHCI, CD3ζ, is expressed in RGCs and CD3ζ deficient mice have reduced RGC dendritic motility, an increase in RGC dendritic density and a selective defect of glutamate receptor-mediated synaptic activity in the retina. The disrupted RGC synaptic activity and dendritic motility is associated with a failure of eye-specific segregation of RGC axon projections to the CNS. These results provide direct evidence of an unrecognized requirement for immune proteins in the developmental regulation of RGC synaptic wiring, and indicate a possible retinal origin for the disruption of eye-specific segregation found in immune deficient mice.

Introduction

Recent studies suggest that genes typically associated with the immune system, such as those in the major histocompatibility complex, are expressed by neurons in various regions of the central nervous system (CNS) and may play important roles in synapse formation (Corriveau *et al*., 1998; Huh *et al*., 2000; Ishii *et al*., 2003; Syken and Shatz, 2003; Syken *et al*., 2006; Baudouin *et al*., 2008). Synaptic circuits in the visual system, particularly eye-specific retinogeniculate projections, have proven to be an excellent model for these studies. Genetic deletion or mutation of a number of MHC class I genes (MHCI), including β2-microglobulin, a MHCI cosubunit; or CD3ζ, a key component of MHCI receptors; result in the failure of eye-specific segregation of retinal ganglion cell (RGC) axon projections to the dorsal lateral geniculate nucleus (dLGN) (Huh *et al*., 2000). In addition, genetic deletion of MHCI molecules enhances long-term potentiation (LTP) and abolishes long-term depression (LTD) in hippocampus (Huh *et al*., 2000) and increases the frequency of spontaneous

*To whom correspondence should be addressed. Tel: (801) 213-2852, Fax: (801) 587-8314, ning.tian@hsc.utah.edu.

'miniature' synaptic currents (mEPSCs) in hippocampal and cortical neurons (Goddard *et al*., 2007). Furthermore, spatial learning, memory, and neurogenesis in hippocampus are markedly reduced in immune-deficient mice (Ziv *et al*., 2006), strongly suggesting that a common immune-associated mechanism might regulate various aspects of activity-dependent synaptic development and plasticity in the CNS.

Activation of immune molecules in neurons could produce similar intracellular signals as those generated in immune cells but with different ultimate effect, such as altering synaptic development, strength, neuronal morphology or circuit properties downstream of synaptic activity (Boulanger *et al*., 2001; Fourgeaud and Boulanger, 2007; Syken *et al*., 2006). For instance, in the immune system activation of CD3ζ regulates immune cell morphology by reorganizing the actin-based cytoskeleton (Baniyash, 2004). Similarly, direct activation of CD3ζ on hippocampal neurons affects cell morphology by promoting dendritic pruning through a tyrosine-based phosphorylation signaling motif common to the immune system (Baudouin *et al*., 2008). Alternatively, MHCI proteins in neurons may interact with non-immune-proteins through non-classical signaling pathways (Ishii et al., 2003; Ishii and Mombaerts, 2008). We sought to shed light on the role of MHCI proteins in the CNS by examining whether and how genetic mutation of CD3ζ affects RGC dendritic pruning, synaptic activity and eye-specific segregation during development.

Numerous reports show that both the developmental segregation of eye-specific projections of RGC axons to the dLGN and the laminar-specific distribution of RGC dendrites in the retina are regulated by retinal synaptic activity (Akerman *et al*., 2002; Bansal *et al*., 2000; Bodnarenko *et al*., 1993; Chapman, 2000; Grubb *et al*., 2004; Huberman et al., 2003; Muir-Robinson *et al*., 2002; Penn *et al*., 1998; Rossi *et al*., 2001; Shatz and Stryker, 1988; Torborg *et al*., 2005; Tian and Copenhagen, 2003; Wong *et al*., 2000; Wong and Ghosh, 2002; Xu and Tian, 2007). Recent studies examining immune deficient mice found that abnormalities in RGC eye-specific segregation are not associated with functional retinal defects during the first postnatal week and therefore concluded that abnormal retinogeniculate projections are due to a loss of immune protein-mediated signaling in the dLGN (Huh *et al*., 2000;). However, it is well documented that retinal activity during early postnatal development is mediated by two major excitatory neurotransmitters, acetylcholine during the first postnatal week and glutamate thereafter (Bansal *et al*. 2000; Demas *et al*. 2003; Feller *et al*. 1996; Zhou 2001). Pharmacological or genetic blockade of either cholinergic or glutamatergic retinal synaptic activity perturbs the development of eye-specific segregation of RGC axonal projections to the dLGN (Rossi *et al*., 2001; Chapman, 2000; Grubb *et al*., 2004; Muir-Robinson *et al*., 2002; Penn *et al*., 1998; Torborg *et al*., 2005). Therefore, it remains unanswered whether retinal activity mediated by glutamate receptors (GluRs) during the second postnatal week is impaired in immune deficient mice, and whether this impairment plays a role in eye-specific segregation defects in these mice. A further goal of the present study is to determine whether genetic mutation of CD3ζ affects the development of retinal synaptic circuitry.

Accordingly, we examined the development of RGC dendritic/axonal structure and synaptic activity in wild type (WT) mice and mice with genetic mutation of CD3ζ (CD3ζ-/- mice). We reveal a previously unidentified mechanism by which CD3ζ regulates the formation of RGC synapses in both retina and dLGN. Our data shows that CD3ζ is preferentially expressed by neurons in the RGC layer of the retina. In CD3ζ-/- mice, the kinetics of RGC dendritic elimination is markedly reduced and the number of dendritic protrusions is significantly increased during early postnatal development. Application of GluR antagonists to developing WT retinas mimics the RGC dendritic defects of CD3ζ-/- mice, confirming the synaptic origin of the dendritic phenotypes in CD3ζ mutants. In mature CD3ζ mutants, RGCs have increased dendritic density, wide-spread dendritic ramifications in the inner

plexiform layer (IPL), and retarded segregation of RGCs dendrites into ON and OFF synaptic pathways. In addition, the strength of spontaneous retinal activity mediated by GluRs during the second postnatal week, but not that mediated by nicotinic AChRs during the first postnatal week, is selectively reduced. Consistent with this, the activity-dependent eye-specific segregation of RGC axonal projections in dLGN is normal at the end of the first postnatal week but fails to improve during the second postnatal week in CD3ζ mutants, suggesting that the dominant phenotypes described in the dLGN of CD3ζ-/- mice are a downstream effect of the deficiencies in GluR-mediated synaptic activity in the retina. Furthermore, light-evoked GluR-mediated responses of RGCs and amacrine cells (ACs) in immature CD3ζ mutants are reduced without significant change of presynaptic bipolar cell (BC) light response, suggesting that in the visual system the initial site of CD3ζ-mediated effects is at synapses between BCs and RGCs. In total, these results directly demonstrate that CD3ζ regulates synaptic wiring and selectively impairs GluR-mediated synaptic activity in the retina during development.

Results

RGCs of CD3ζ-/- mice have altered dendritic structure in developing retina

We first examined the expression of CD3ζ in the developing mouse retina. We observed strong CD3ζ immunoreactivity mainly in the inner retina, including both cells located in the RGC layer and IPL, in both developing and more mature mice (Fig 1A). Double labeling of CD3ζ with RGC or AC markers revealed that most, if not all, Brn3b-positive RGCs are CD3ζ positive (Fig 1B), as are many displaced ACs located in the RGC layer (labeled by the pan-AC antibody, Pax6). However, most ACs in the inner nuclear layer (INL), labeled with the same antibody, are CD3ζ negative (Fig 1B). *In situ* hybridization confirmed the expression of CD3ζ mRNA in the RGC layer in both developing (P14) and more mature (P28) mice. To further investigate the synaptic localization of CD3ζ in the retina, we performed double immunostaining using antibodies against CD3ζ and synaptic markers. We observed many CD3ζ-positive puncta that colocalized with the postsynaptic protein PSD95 in the IPL (Fig 1C). We also found that many CD3ζ-positive puncta in the IPL were closely associated with the presynaptic ribbon protein, CtBP2, in both young and more mature retinas (Fig 1D). Taken together, these findings demonstrate that CD3ζ is preferentially expressed by retinal neurons located in the RGC layer in the developing retina and is localized at synapses in the IPL during the period of synaptic formation. In addition, we used RT-PCR to confirm that retinal neurons in CD3ζ-/- mice express only a truncated mRNA of the gene (CD247) encoding CD3ζ protein. Exons 2 and 3 of the CD247 gene are not expressed in this truncated mRNA (Fig 1E), which is consistent with previous reports on immune cells in CD3ζ-/- mice (Love *et al*., 1993).

Recent studies reported that immune deficient mice, including CD3ζ-/- mice, have defects in eye-specific segregation of RGC axon projections to the dLGN (Huh *et al*., 2000). We therefore examined whether genetic mutation of CD3ζ affects the structure of RGC dendrites as well. To visualize the fine dendritic structure of RGCs, we used a line of transgenic mice in which Yellow Fluorescent Protein (YFP) is expressed in a small fraction of RGCs (Feng *et al*., 2000). At P12, RGC dendrite morphology in YFP+/CD3ζ-/- mice was very different than littermate controls, particularly in the number of dendritic protrusions (Fig 2A). We classified YFP+ RGCs into 12 morphological subtypes following the approach developed by Sun et al. (2002) and Diao et al. (2004), which is based on the soma size, dendritic field size, dendritic stratification level in the IPL, and branching pattern of RGCs. Although the total branch number is increased, RGC soma and dendritic field size as well as dendritic stratification level in the IPL are well conserved (see below), making RGC subtype classification straight-forward for CD3ζ-/- mice. We manually traced and quantified the dendritic branches of two RGC morphological subtypes (A1 and A2). On average, the

number of dendritic protrusions of both A1 and A2 RGCs in CD3ζ-/- mice are 6-fold higher than that of age-matched WT controls (Fig 2B). A similar increase in dendritic protrusions was found in other RGC subtypes (Fig S1). In addition, the density of dendritic protrusions in both A1 and A2 RGCs of CD3ζ+/- mice are significantly higher than that of WT mice, but much lower than that of CD3ζ-/- mice (Fig 2B), suggesting a gene dosage effect. We also examined the dendritic density of all morphological subtypes of RGCs using Sholl analysis (Fig 2C) (Sholl, 1953) and found that the dendrites of 4 (B2, B3, C1 and C5) out of a total of 12 morphological RGC subtypes were significantly denser than that of age-matched WT controls (Fig 2D), without a change in the size of the overall dendritic field (DF) (Fig 2E). Taken together, these results clearly demonstrate that genetic mutation of CD3ζ affects the dendritic structure of RGCs in developing retina.

Dendritic motility of RGCs in CD3ζ-/- mice is reduced

To gain more insight into why dendritic pruning of RGCs during development is perturbed in CD3ζ mutant mice, we directly examined the kinetics of RGC dendritic growth and elimination in retinas from P12/P13 mice using time-lapse confocal microscopy (Movie S1). Fig 3B shows maximum projection images of a dendritic segment from the YFP-expressing A1 RGC shown in Fig 3A at different points in time. Addition, elimination, extension and retraction of dendritic protrusions are all evident in these images, demonstrating the high motility of RGC dendritic protrusions.

By tracking dendritic protrusions over time, we found that the speed of extension and retraction were reduced by 40-42% in CD3ζ-/- RGCs in comparison to WT controls (Fig 3C). The reduction of RGC dendritic motility is associated with a significant increase in the lifetime of RGC dendritic protrusions. In WT RGCs, 31.8 ± 2.9% of the dendritic protrusions were replaced within one hour while only 15.4 ± 3.3% of the dendritic protrusions were replaced in one hour in CD3ζ-/- RGCs. On the other hand, RGCs of CD3ζ-/- mice have twice as many dendritic protrusions with long lifetimes (> 5.5 hours) in comparison with that of WT mice (Fig 3D). These results demonstrate that genetic mutation of CD3ζ affects RGC dendritic pruning by regulating the kinetics of RGC dendrite motility.

Changes in RGC dendritic motility in developing CD3ζ-/- retina alter dendritic structure and synaptic connectivity in mature RGCs

We wondered whether alterations in dendritic motility of developing CD3ζ-/- RGCs cause permanent defects in retinal synaptic wiring in more mature mice. We examined dendritic structure of RGCs in more mature CD3ζ-/- mice and littermate controls (Fig 4). As in the developing retina, RGC dendritic density in P33 CD3ζ-/- mice is much higher than that of WT controls (Fig 4A). Both A1 and A2 RGCs in CD3ζ-/- mice have significantly higher dendritic density as reflected in both dendritic length (Fig 4B) and the total number of dendritic branches (Fig 4C). Interestingly, the increase in dendritic density was restricted to higher order dendritic branches (Fig 4D and 4E). Sholl analysis of all morphological subtypes of P33 RGCs showed that the total number of dendritic crossing points in RGCs of CD3ζ-/- mice was significantly higher (Fig 4F and 4G, $p<0.0001$, K-S test). A more detailed analysis revealed that the dendritic densities are much higher for nearly all RGC morphological subtypes in CD3ζ-/- mice (Figs 4I and S2), although the dendritic field sizes were not different from that of WT controls (Fig 4H).

The developmental defects in RGC dendritic motility also significantly compromised RGC dendritic stratification in more mature (P33) CD3ζ-/- mice (Fig 5). The RGC dendritic width in 9 of 12 subtypes in CD3ζ-/- mice was significantly larger (Fig 5C), while the average dendritic width across all subtypes was 40% greater in CD3ζ-/- mice than in WT controls (Fig 5B). The increase in dendritic width is not due to a vertical expansion of IPL thickness

in mutant mice (IPL thickness of P34 WT, CD3ζ+/- CD3ζ-/- mice are 63.39 ± 2.05 μm, 65.82 ± 8.04 μm and 63.49 ± 2.87 μm; mean ± SE, n = 4 for each group, p = 0.929, ANOVA test). As a result of their greater dendritic spread, RGCs in CD3ζ-/- mice were more likely to have dendrites in both OFF and ON sublamina of the IPL. Quantitatively (Fig 5D), we observed a significant decrease in the fraction of RGCs with dendrites confined to either the ON sublamina (n=71/164 in WT, n=55/161 in CD3ζ-/-, $p < 0.05$), or OFF sublamina (n=36/164 in WT, n=15/161 in CD3ζ-/-, $p < 0.01$) in CD3ζ-/- mice, and a large and significant increase in the fraction of cells with dendrites that spanned both ON and OFF sublamina in CD3ζ-/- mice (n=57/164 in WT, n=91/161 in CD3ζ-/-, $p < 0.01$).

To directly test whether more RGCs in CD3ζ-/- mice receive functional synaptic inputs from both ON and OFF BCs, we recorded RGC light evoked responses in P30 mice using a multi-electrode array (MEA) system (Tian and Copenhagen, 2003). RGCs were divided into ON, OFF and ON-OFF cells based on their light response patterns (Fig 5E). ON cells generated visually identifiable increases in spike frequency when the light was turned on. OFF cells produced an increase in spiking only following the termination of the stimulus. ON-OFF cells exhibited increased spike activity following both the onset and the termination of the light stimulus. Consistent with the morphological findings that RGCs of CD3ζ-/- mice ramify their dendrites more diffusely, with many of them extending into both ON and OFF sublaminae of the IPL, there were 16% fewer ON responsive RGCs in CD3ζ-/- mice compared to WT controls (Fig 5F; n=396/700 in WT, n=231/570 in CD3ζ-/-, $p < 0.05$) and 70% more ON-OFF responsive RGCs in CD3ζ-/- mice compared to WT controls (Fig 5F; n=202/700 in WT, n=276/570 in CD3ζ-/-, $p < 0.0001$).

GluR-mediated synaptic transmission is selectively reduced in the inner retina of developing CD3ζ mutants

Previous studies reported that immune deficient mice have abnormal eye-specific segregation of RGC axonal projections to the dLGN without any functional abnormalities in the retina during the first postnatal week. It was therefore concluded that the abnormal retinogeniculate projections are due to a loss of immune molecule-mediated signaling in the dLGN (Huh *et al*., 2000; Stevens *et al*., 2007). However, retinal synaptic activity during early postnatal development is mediated by both AChRs and GluRs, with a developmental shift from cholinergic to glutamatergic synaptic transmission during the middle of the second postnatal week in mice (Bansal *et al*. 2000; Demas *et al*. 2003; Feller *et al*. 1996; Zhou 2001). Moreover, activity mediated by both AChRs and GluRs is critical for the development and maintenance of eye-specific segregation of RGC axonal projections to the dLGN (Rossi *et al*., 2001; Chapman, 2000; Grubb *et al*., 2004; Muir-Robinson *et al*., 2002; Penn *et al*., 1998; Torborg *et al*., 2005).

We therefore investigated whether genetic mutation of CD3ζ affects glutamatergic synaptic activity in the developing retina. We examined spontaneous retinal wave activity mediated by AChRs at P3 and GluRs at P10 in WT, CD3ζ+/- and CD3ζ-/- mice using MEA recordings (Fig 6A). At P3, spontaneous retinal waves mediated by nAChRs were indistinguishable in WT, CD3ζ+/- and CD3ζ-/- retinas (Fig 6B, 6D and 6E). At P10, however, the frequency of retinal waves was significantly reduced in the CD3ζ-/- mice compared to controls (WT and CD3ζ+/-; Fig 6D). Pharmacological blockade of GluRs by bath application of NBQX and AP5 largely blocks retinal wave activity in both WT and CD3ζ mutants at P10 (Fig 6E), confirming that retinal waves at this age are dominated by GluR-mediated synaptic activity in both WT and CD3ζ mutants, though they are reduced in frequency in CD3ζ mutants.

We recorded light evoked synaptic activity with *in vivo* electroretinogram (ERG) measurements to further examine whether mutation of CD3ζ specifically affects GluR-

mediated synaptic function in the inner retina of immature animals. A typical ERG waveform consists of three major components, an a-wave, a b-wave and oscillatory potentials (OPs) (Fig 6H). The a-wave of the ERG is a measure of photoreceptor function, while the b-wave of the ERG is a measure of ON bipolar cell function and reflects both photoreceptor and synaptic function in the outer plexiform layer of the retina (Stockton and Slaughter, 1989). The OPs, which reflect interactions among bipolar, amacrine, and ganglion cells, is a measure of inner retinal function (Wachtmeister, 1998). We found that the light evoked responses of inner retinal neurons (RGCs and ACs) of CD3ζ-/- mice at P14, measured as OPs of the ERG, were significantly reduced (Fig 6G) while the light response of photoreceptors (data not shown) and ON BCs, measured as the amplitudes of the ERG b-wave, were nearly identical to that of P14 WT mice (Fig 6G). This demonstrates that GluR-mediated synaptic transmission in the inner retina is specifically compromised in immature CD3ζ-/- mice. Furthermore, we examined the ERG of more mature (P30) CD3ζ-/- mice (Fig 6H). Consistent with the results from P14 CD3ζ-/- mice, the light responses of photoreceptors and ON BCs of P30 CD3ζ-/- mice are not different from that of age-matched WT controls (Fig 6I). However, CD3ζ mutants have significantly enhanced, but not reduced, inner retinal neuron light response in more mature mice (Fig 6J). Taken together, these results clearly demonstrate that genetic mutation of CD3ζ preferentially affects GluR-mediated synaptic transmission in the retina.

GluR-mediated synaptic activity regulates RGC synaptic formation likely through CD3ζ-mediated signaling

GluR mediated spontaneous retinal activity during the second postnatal week is thought to drive fine eye-specific segregation in the mouse since defects in glutamatergic neurotransmission in the retina during this period affect central projections of RGCs to the dLGN (Demas et al., 2006). To explore the relationship between retinal synaptic activity and RGC dLGN projections in CD3ζ-/- mice, we examined eye-specific segregation of RGC axonal projections in the dLGN of CD3ζ-/- mice at P8, which is the time GluR-mediated retinal waves start to replace waves mediated by nAChRs. We found that eye-specific segregation is normal at P8 in CD3ζ-/- mice, but at P16, after a week of GluR-mediated retinal waves, eye-specific segregation of RGC axonal projections to the dLGN fails to improve in CD3ζ-/- mice, as it does in WT mice (Fig 7A, 7B). The eye-specific segregation defects in CD3ζ-/- mice persist until at least P35 (Fig S3), showing that mutation of CD3ζ likely causes permanent defects in eye-specific segregation. These results suggest that the RGC axon projection abnormalities observed in CD3ζ-/- mice are the result of defects in glutamatergic synaptic activity in the retina, not the loss of CD3ζ in the dLGN.

The expression of immune proteins by neurons in the CNS is regulated by neuronal activity (Corriveau *et al*., 1998; Huh *et al*., 2000), which suggests that synaptic activity regulates the morphological development of neurons through immune molecule-mediated signaling. To test this hypothesis, we blocked GluR-mediated synaptic activity in WT mice with daily injections of NBQX+AP5 into both eyes from P7 to P12. We found that NBQX+AP5 treatment resulted in disrupted eye-specific segregation at P14 compared with saline treated control animals (Fig 8A-E), consistent with a specific role of retinal GluRs mediating RGC axon refinement in the dLGN. We also examined the effects produced by applying GluR antagonists during development on RGC dendritic structure in WT and CD3ζ-/- retinas. Intraocular injection of GluR antagonists NBQX (40 μM) and AP5 (400 μM) into one eye of WT mice from P7-11 (once a day for 5 days) to suppress GluR-mediated retinal synaptic activity resulted in a significant increase in the density of dendritic filopodia at P12 (Fig 8F), similar to that seen in CD3ζ-/- mice (Fig 2B). However, intraocular injection of NBQX and AP5 into the eyes of CD3ζ-/- mice had no additional effect on the density of RGC dendritic filopodia (Fig 8F and Fig 2B). Moreover, bath application of NBQX (10 μM) and AP5 (100

μM) on WT retinas reduced RGC dendritic motility to the same degree as that observed in CD3ζ-/- mice (Fig 8G, 8H). These results strongly support the idea that GluR-mediated synaptic activity regulates RGC dendritic structure and motility through CD3ζ-mediated signaling.

Discussion

We have presented strong evidence that the immune molecule CD3ζ participates in the activity-dependent synapse formation of RGCs in both the retina and dLGN. We showed that CD3ζ is specifically expressed by RGCs and displaced ACs, and that CD3ζ-/- mice exhibit a profound alteration in RGC dendritic motility in immature animals, a loss of lamina-specific segregation of RGC dendrites in the IPL, and a permanent defect in RGC axonal projections to the dLGN. These defects are associated with a selective reduction in GluR-mediated retinal synaptic activity during the second postnatal week. These results provide the first direct evidence that GluR-mediated synaptic activity regulates synaptic formation in the CNS through an immune molecule-mediated signaling pathway.

CD3ζ selectively regulates GluR-mediated synaptic transmission of RGCs in early postnatal development

It is striking that glutamatergic synaptic transmission in the inner retina is selectively impaired in CD3ζ-/- mice. Evidence for this comes from two very distinct approaches. First, we showed that GluR-mediated retinal waves during the second postnatal week are disrupted in the CD3ζ-/- mice, but retinal waves mediated by nAChRs during the first postnatal week are unaffected. Our results are consistent with previous reports that mutation of CD3ζ and other immune molecules does not alter retinal synaptic activity during the first postnatal week (Huh *et al*., 2000; Stevens *et al*., 2007), but these investigators did not examine GluR-mediated retinal waves in the second postnatal week. Second, we showed that inner retina light evoked synaptic activity measured with ERGs is specifically compromised in CD3ζ-/- mice, while GluR-mediated synaptic transmission between photoreceptors and ON BCs is normal. Moreover, we showed that CD3ζ is strongly expressed in the dendrites of RGCs and colocalizes with presynaptic and postsynaptic markers in the IPL. Therefore, not only do we describe how the effects induced by CD3ζ mutation are specific to GluR-mediated synaptic transmission, we also show that glutamatergic neurons that do not express CD3ζ are not directly affected. It is worth noting that many displaced ACs, including cholinergic displaced ACs, express CD3ζ. Although genetic mutation of CD3ζ does not seem to affect synaptic activity mediated by these cells, it remains unknown whether CD3ζ regulates the dendritic structure of these ACs.

Do the CNS defects in immune deficient mice originate in the retina?

Another surprising and intriguing finding from this study is that eye-specific RGC axon segregation defects in the dLGN of CD3ζ-/- mice appear to share the same time course as defects in GluR-mediated retinal waves. It is well documented that retinal activity is crucial for the normal development of synaptic connections in the retina, dLGN, superior colliculus and visual cortex. Blocking spontaneous or light evoked retinal activity retards the emergence of RGC dendritic stratification in the retina (Bansal *et al*., 2000; Bodnarenko *et al*., 1993; Tian and Copenhagen, 2003; Wong *et al*., 2000; Wong and Ghosh, 2002; Xu and Tian, 2007), eye-specific segregation and retinotopic map of RGC axonal projections to the dLGN (Rossi *et al*., 2001; Akerman *et al*., 2002; Chapman, 2000; Grubb *et al*., 2004; Huberman *et al*., 2003; Muir-Robinson *et al*., 2002; Penn *et al*., 1998; Shatz and Stryker, 1988; Torborg *et al*., 2005; Grubb *et al*., 2004) and superior colliculus (Rossi *et al*., 2001; Chandrasekaran *et al*., 2005; McLaughlin *et al*., 2003; Mrsic-Flogel *et al*., 2005), the development of precise dLGN projections to visual cortex (Stryker and Harris, 1986; Cang

et al., 2005; Huberman *et al*., 2006), and the dendritic/axonal growth of neurons in the visual system (Majewska and Sur, 2003; Oray *et al*., 2004; Parnavelas *et al*., 1973; Riccio and Matthews, 1985; Wallace and Bear, 2004). This immediately raises the possibility that the dominant phenotypes described in the dLGN of CD3ζ-/- and other MHCI deficient mice (Huh *et al*., 2000) are a downstream effect of the deficiencies in GluR-mediated synaptic activity in the retina, and argues against the current 'standard' model (Huh *et al*., 2000; Boulanger *et al*., 2001) that MHCI molecules directly regulate synaptic wiring in the dLGN.

In addition to reducing both spontaneous and light evoked RGC synaptic activity around the time of eye opening, genetic deletion/mutation of CD3ζ or other MHCI molecules significantly impairs the development of retinogeniculate projections, synaptic strength in the visual cortex, and activity-dependent synaptic plasticity in hippocampus (Huh *et al*., 2000). Since the anatomical and functional defects in the retinogeniculate projections in CD3ζ mutants and mice with mutations of other MHCI molecules (Goddard *et al*., 2007; Huh *et al*., 2000) are very similar to that induced by deprivation of retinal synaptic activity (Akerman *et al*., 2002; Grubb *et al*., 2004; Huberman *et al*., 2003; Muir-Robinson *et al*., 2002; Penn *et al*., 1998; Shatz and Stryker, 1988; Torborg *et al*., 2005; Hooks and Chen, 2006), it is likely that changes in RGC synaptic activity in the CD3ζ mutants have significant impact on eye-specific segregation of RGC axonal projections in the dLGN. Consistent with this idea, our results show clear and obvious eye-specific segregation at P8 in both WT and CD3ζ-/- mice, demonstrating that CD3ζ mutation has minimum effect on retinogeneculate mapping during the first postnatal week. The similarity between the segregation defects found in WT mice treated with NBQX+AP5 after P7 and CD3ζ-/- mice at P16 strongly suggests a failure of activity-dependent axon maintenance/refinement during the second postnatal week.

Obviously, our results do not rule out a role for immune molecule-mediated signals in the regulation of synaptic structure and function in areas of the CNS beyond the retina. The mRNA and proteins of several members of the MHCI family are expressed in various regions of the CNS in addition to the retina, including dLGN, brainstem motoneurons, nigral dopaminergic neurons, developing and adult hippocampal pyramidal neurons and cortical pyramidal neurons (Corriveau *et al*., 1998; Huh *et al*., 2000; Ishii *et al*., 2003; Linda *et al*., 1999; Syken and Shatz, 2003; Syken *et al*., 2006). The expression of these molecules often occurs in regions of the brain at times when development is highly regulated by neural activity (Corriveau *et al*., 1998; Huh *et al*., 2000). The structural and functional changes in synaptic connections in these CNS neurons induced by genetic deletion of MHCI molecules, such as the increase in the frequency of sEPSCs, enhanced LTP and the absence of LTD in the hippocampus (Huh *et al*., 2000; Goddard *et al*., 2007), are unlikely related to changes in RGC synaptic activity. Therefore, it remains possible that immune molecules directly regulate the development of synapses in higher centers of the visual system and other parts of the CNS beyond the retina. Further experiments in which MHCI molecule expression is locally manipulated in specific regions of the visual system and CNS are necessary to help distinguish the various possibilities.

The enhanced light evoked inner retinal responses we observed in more mature CD3ζ-/- retinas, reflected by increased ERG amplitudes, suggests that synaptic transmission in the inner retina is also enhanced in the adult. This may be the result of increased RGC dendritic density and synaptic contacts between RGCs and BCs. A similar enhancement of synaptic transmission was reported previously in other parts of the CNS after genetic deletion of MHCI molecules (Huh *et al*., 2000; Goddard *et al*., 2007). The enhanced synaptic transmission in various parts of the CNS in adult immune deficient mice may very well be a secondary effect of the defects in synaptic elimination during early postnatal development.

How do immune molecules regulate neuronal synaptic wiring?

It remains unknown how immune molecule-mediated signals interact with GluR-mediated synaptic activity in the regulation of neuronal synaptic wiring. The fact that mice deficient in a variety of MHCI molecules, such as CD3ζ and βm/TAP1, have very similar retinogeniculate projection phenotypes implies that immune molecules function in the CNS via a common molecular pathway (Boulanger *et al*., 2001, 2004; Huh *et al*., 2000). Mechanistically, it was postulated that immune molecules in neurons engage with MHCI receptors expressed on neurons or non-neural cells in the CNS, generating common intracellular signals in both neurons and immune cells that ultimately alter synaptic strength, neuronal morphology and circuit properties downstream of synaptic activity (Boulanger *et al*., 2001; Fourgeaud and Boulanger, 2007; Syken *et al*., 2006). Consistent with this, genetic deletion of β2m/TAP1 reduces surface expression of MHCI on hippocampal and layer 4 cortical neurons. In addition, β2m/TAP1 mutant mice have increased mini-EPSC frequency, enhanced LTP but no LTD, and larger presynaptic boutons and vesicle numbers in the hippocampus, suggesting that MHCI acts retrogradely across the synapse (Huh *et al*., 2000; Boulanger *et al*., 2001; Goddard *et al*., 2007).

However, our results show that altered RGC axon projections to the dLGN and aberrant RGC dendritic ramification in the retina are associated with a profound reduction, not enhancement, of GluR-mediated synaptic activity in young CD3ζ-/- mice. Moreover, many of the structural RGC dendrite defects observed in immature CD3ζ-/- mice are phenocopied by pharmacologically blocking GluR-mediated synaptic transmission in the retina of WT mice. These results suggest that activation of CD3ζ-mediated signals normally associates with enhancement of GluR-mediated synaptic transmission. Pharmacological blockade of GluR-mediated synaptic activity in CD3ζ-/- mice had no effect on RGC dendritic structure beyond that already observed in CD3ζ-/- mice alone, suggesting that GluR-mediated synaptic activity and CD3ζ-mediated signals regulate RGC dendritic structure through the same synaptic mechanism. The fact that CD3ζ mutation only reduces GluR-mediated synaptic transmission of inner retinal neurons in immature mice also strongly suggests that activity of CD3ζ-mediated signals specifically associates with GluR-mediated synaptic transmission in a cell- and time-dependent manner. Given that the expression of immune molecules is regulated by GluR-mediated synaptic activity in the CNS (Corriveau *et al*., 1998; Huh *et al*., 2000), and the activation of CD3ζ in immune cells regulates dendritic growth and cell migration through the control of actin-based cytoskeletal reorganization (Baniyash, 2004), it is possible that the function of CD3ζ in RGCs is regulated by GluR-mediated synaptic activity and CD3ζ couples short-term changes in synaptic strength with long-term cytoskeletal changes in RGC axons and dendrites. Pharmacological blockade of GluR-mediated synaptic activity had no additional affect on RGC morphology beyond that already observed in CD3ζ-/- mice, consistent with the idea that CD3ζ-mediated signals function downstream of GluR-mediated synaptic activity in regulating RGC development.

Material and methods

Animals

Thy1-YFP+ and CD3ζ-/- mice, both on a C57BL/6 background, were obtained from The Jackson Laboratory (Bar Harbor, ME). Thy1-YFP+/CD3ζ+/- mice were first generated by crossing Thy1-YFP+ and CD3ζ-/-. Then, Thy1-YFP+/CD3ζ-/- mice were generated by Thy1-YFP+/CD3ζ+/- mating. No difference was found between Thy1-YFP+ and littermate Thy1-YFP+/CD3ζ+/+, so both were used as controls in this study. The handling and maintenance of animals met NIH guidelines and was approved by Yale's Institutional Animal Care and Use Committee.

Preparation of retinal whole-mounts and retina sections for fluorescent imaging and *in situ* hybridization

Standard protocols for retinal whole-mount and cross section preparations for fluorescent (Xu and Tian, 2007; 2008) and *in situ* hybridization (Li and Joyner, 2001) were used as described previously. See Supplement Data for details.

Morphological classification of RGCs

The method for morphological classification of RGCs follows the approach developed by Sun et al. (2002) and Diao et al. (2004). See Supplement Data for details.

RT-PCR

Retina tissues were collected from CD3ζ+/+, CD3ζ+/- and CD3ζ-/- mice, respectively. Total RNA was extracted using TRIzol Reagent (Invitrogen). 2 μg of RNA were reversed transcribed using oligo (dT) (Invitrogen) as primer for 1 hour with SuperScript III Reverse Transcriptase (Invitrogen). 2 μl of the RT-reaction mixture were taken for PCR with the primers as follows: CD247 exon1-F, 5'-TGT CAG CCA CAG AAC AAA GC-3'; CD247 exon3-R, 5'-TGC ACT CCT GCT GAA TTT TG-3'; CD247 exon4-R, 5'- CTC TTC GCC CTA GAT TGA GC-3'; CD247 exon6-F, 5'-CCT ACA GTG AGA TCG GCA CA-3'; CD247 exon8-R, 5'-GTC CAG GGA TGA CGT TCT GT-3'; Oct1 exon15-F, 5'- CTG CTG GAG GTG CCT TAC TC-3'; Oct1 exon17-R, 5'-CAG GAA CAG AGG TGC AGT CA-3'; GAPDH exon1-F, 5'-AGT GCC AGC CTC GTC CCG TA-3'; GAPDH exon4-R, 5'-TGA GCC CTT CCA CAA TGC CA-3'. The amplification yields 293 bp (CD247 1F/3R), 357 bp (CD247 1F/4R), 314 bp (CD247 6F/8R), 206 bp (Oct1 15F/17R), and 543 bp (GAPDH 1F/4R) for the WT gene, respectively. PCR products were separated in a 2% agarose gel and stained with ethidium bromide.

Time-lapse imaging of RGC dendrites

The time-lapse images of RGCs were taken from whole-mount retina preparations. Retinas with YFP-expressing RGCs were isolated in oxygenated extracellular solution that contained (in mM) NaCl 124, KCl 2.5, $CaCl_2$ 2, $MgCl_2$ 2, NaH_2PO_4, 1.25, $NaHCO_3$ 26 and glucose 22 (pH 7.35 with 95% O_2 and 5% CO_2), mounted on nitrocellulose filter paper (Millipore Corp), placed in a recording chamber and continuously perfused at 31.5°C. Time-lapse images were taken every 30 minutes for 6 hours.

ERG recordings

The ERG recording procedures have previously been described (Vistamehr and Tian, 2004). See Supplement Data for details.

Multielectrode array (MEA) recordings

The procedures of MEA recording and retinal wave characterization have previously been described (Tian and Copenhagen, 2003; Torborg *et al*., 2005; Wong *et al*., 1993). See Supplement Data for details.

Intraocular injection and LGN image analysis

The procedure of intraocular injection and dLGN image analysis have been described previously. Briefly, Alexa Fluor 555- and 647-conjugated β-Cholera toxin (1 μl) or Alexa Fluor 488- and 594-conjugated β-Cholera toxin were injected into the right and left eye, respectively, at either P6 or P14 for the study of eye-specific segregation. Brains were dissected, fixed and sectioned 48 hours after injection. Three continuous brain sections that contained the largest ipsilateral projection were selected for imaging (Chandrasekaran, et al.,

2005). Eye-specific segregation in the dLGN was determined as the fraction of contra-projection, ipsi-projection and overlapped projections in the dLGN (Torborg and Feller, 2004; Torborg, *et al*, 2005) and Segregation Index (Torborg and Feller, 2004; Torborg, *et al*, 2005). See Supplement Data for details.

The injection of GluR antagonists and saline followed the same protocol as described above. Briefly, NBQX (40 μM) and AP5 (400 μM) were injected daily from P7 to P11 or P12. Each eye received about 0.5 μl per day. For eye segregation experiments, NBQX and AP5 were injected into both eyes and the control animals received the same amount of saline injections binocularly. For the filopodia studies, one eye was injected with NBQX+AP5 and another eye was injected with saline for comparison.

Statistical analysis

The Kolmogorov-Smirnov (K-S) test was used to determine the significance of differences in the cumulative distributions. ANOVA and Student's *t*-test were used to examine the difference between two or more means using StatView (Abacus Concepts) software. All data presented in this study are mean ± SD in the text and mean ± SEM in the figures except specified.

Supplementary Material

Refer to Web version on PubMed Central for supplementary material.

Acknowledgments

This work was supported by NIH grants R01EY012345 and P30 EY000785, Research to Prevent Blindness (RPB) and Funds from the Connecticut Lion, Eye Research Foundation (N. Tian), James Hudson Brown-Alexander B. Coxe Fellowship from Yale University (H. P. Xu), NIH grants R01EY015788 and P30EY000785 (M. Crair), and NIH grant R01EY013426 (L. Gan). We wish to thank Dr. Nigel Daw for critical reading of the manuscript. We also thank Dr. Zhinan Yin for critical discussion, Dr. Susumu Tomita and Ms. Yueyi Zhang for technical support.

References

Akerman CJ, Smyth D, Thompson ID. Visual experience before eye-opening and the development of the retinogeniculate pathway. Neuron 2002;36:869–879. [PubMed: 12467590]

Baniyash M. TCR zeta-chain downregulation: curtailing an excessive inflammatory immune response. Nat Rev Immunol 2004;4:675–87. [PubMed: 15343367]

Bansal A, Singer JH, Hwang BH, Xu W, Beaudet A, Feller MB. Mice lacking specific nicotinic acetylcholine receptor subunits exhibit dramatically altered spontaneous activity patterns and reveal a limited role for retinal waves in forming ON and OFF circuits in the inner retina. J Neurosci 2000;20:7672–7681. [PubMed: 11027228]

Baudouin SJ, Angibaud J, Loussouarn G, Bonnamain V, Matsuura A, Kinebuchi M, Naveilhan P, Boudin H. The Signaling Adaptor Protein CD3ζ Is a Negative Regulator of Dendrite Development in Young Neurons. Mol Biol Cell 2008;19:2444–2456. [PubMed: 18367546]

Bodnarenko SR, Chalupa LM. Stratification of ON and OFF ganglion cell dendrites depends on glutamate-mediated afferent activity in the developing retina. Nature 1993;364:144–146. [PubMed: 8100613]

Bodnarenko SR, Yeung G, Thomas L, McCarthy M. The development of retinal ganglion cell dendritic stratification in ferrets. Neuroreport 1999;10:2955–2959. [PubMed: 10549804]

Boulanger LM, Huh GS, Shatz CJ. Neuronal plasticity and cellular immunity: shared molecular mechanisms. Curr Opini Neurobiol 2001;11:568–578.

Boulanger LM, Shatz CJ. Immune signaling in neural development synaptic plasticity and disease. Nature Rev Neurosci 2004;5:521–531. [PubMed: 15208694]

Bradke F, Dotti CG. Changes in membrane trafficking and actin dynamics during axon formation in cultured hippocampal neurons. Microsc Res Tech 2000;48:3–11. [PubMed: 10620780]

Cang J, Rentería RC, Kaneko M, Liu X, Copenhagen DR, Stryker MP. Development of precise maps in visual cortex requires patterned spontaneous activity in the retina. Neuron 2005;48:797–809. [PubMed: 16337917]

Chandrasekaran AR, Plas DT, Gonzalez E, Crair MC. Evidence for an instructive role of retinal activity in retinotopic map refinement in the superior colliculus of the mouse. J Neurosci 2005;25:6929–6938. [PubMed: 16033903]

Chapman B. Necessary for afferent activity to maintain eye-specific segregation in ferret lateral geniculate nucleus. Science 2000;287:2479–2482. [PubMed: 10741966]

Clayton LK, D'Adamio L, Howard FD, Sieh M, Hussey RE, Koyasu S, Reinherz EL. CD3eta and CD3zeta are alternatively spliced products of a common genetic locus and are transcriptionally and/or post-transcriptionally regulated during T-cell development. Proc Natl Acad Sci USA 1991;88:5202–5206. [PubMed: 1828894]

Coombs JL, Van Der List D, Chalupa LM. Morphological properties of mouse retinal ganglion cells during postnatal development. J Comp Neurol 2007;503:803–814. [PubMed: 17570502]

Corriveau RA, Huh GS, Shatz CJ. Regulation of class I MHC gene expression in the developing and mature CNS by neural activity. Neuron 1998;21:505–520. [PubMed: 9768838]

Dann JF, Buhl EH, Peichl L. Postnatal dendritic maturation of alpha and beta ganglion cells in cat retina. J Neurosci 1988;8:1485–1499. [PubMed: 3367208]

Demas J, Eglen SJ, Wong RO. Developmental loss of synchronous spontaneous activity in the mouse retina is independent of visual experience. J Neurosci 2003;23:2851–2860. [PubMed: 12684472]

Demas J, Sagdullaev BT, Green E, Jaubert-Miazza L, McCall MA, Gregg RG, Wong RO, Guido W. Failure to maintain eye-specific segregation in nob, a mutant with abnormally patterned retinal activity. Neuron 2006;50:247–259. [PubMed: 16630836]

Diao L, Sun W, Deng Q, He S. Development of the mouse retina: Emerging morphological diversity of the ganglion cells. J Neurobiol 2004;61:236–249. [PubMed: 15389605]

Feller MB, Wellis DP, Stellwagen D, Werblin FS, Shatz CJ. Requirement for cholinergic synaptic transmission in the propagation of spontaneous retinal waves. Science 1996;272:1182–1187. [PubMed: 8638165]

Feng G, Mellor RH, Bernstein M, Keller-Peck C, Nguyen QT, Wallace M, Nerbonne JM, Lichtman JW, Sanes J. Imaging neural subsets in transgenic mice expressing multiple spectral variants of GFP. Neuron 2000;28:41–51. [PubMed: 11086982]

Fisher LJ. Development of synaptic arrays in the inner plexiform layer of neonatal mouse retina. J Comp Neurol 1979;187:359–372. [PubMed: 489784]

Fourgeaud L, Boulanger LM. Synapse remodeling, compliments of the complement system. Cell 2007;131:1034–1036. [PubMed: 18083091]

Goddard CA, Butts DA, Shatz CJ. Regulation of CNS synapses by neural MHC class I. PNAS 2007;104:6828–6833. [PubMed: 17420446]

Grubb MS, Thompson ID. Visual response properties in the dorsal lateral geniculate nucleus of mice lacking the beta2 subunit of the nicotinic acetylcholine receptor. J Neurosci 2004;24:8459–8469. [PubMed: 15456819]

Hooks BM, Chen C. Distinct roles for spontaneous and visual activity in remodeling of the retinogeniculate synapse. Neuron 2006;19:281–291. [PubMed: 17046691]

Huberman AD, Wang GY, Liets LC, Collins OA, Chapman B, Chalupa LM. Eye-specific retinogeniculate segregation independent of normal neuronal activity. Science 2003;300:994–998. [PubMed: 12738869]

Huberman AD, Speer CM, Chapman B. Spontaneous retinal activity mediates development of ocular dominance columns and binocular receptive fields in v1. Neuron 2006;52:247–254. [PubMed: 17046688]

Huh GS, Boulanger LM, Du H, Riquelme PR, Brotz TM, Shatz CJ. Functional requirement for class I MHC in CNS development and plasticity. Science 2000;290:2155–2159. [PubMed: 11118151]

Ishii T, Hirota J, Mombaerts P. Combinatorial coexpression of neural and immune multigene families in mouse vomeronasal sensory neurons. Cur Biol 2003;13:394–400.

Ishii T, Mombaerts P. Expression of nonclassical class I major hitocompatibility genes defines a tripartite organization of the mouse vomeronasal system. J Neurosci 2008;28:2332–2341. [PubMed: 18322080]

Lecuit T, Pilot F. Developmental control of cell morphogenesis: a focus on membrane growth. Nat Cell Biol 2003;5:103–108. [PubMed: 12563275]

Lee T, Winter C, Marticke SS, Lee A, Luo L. Essential roles of Drosophila RhoA in the regulation of neuroblast proliferation and dendritic but not axonal morphogenesis. Neuron 2000;25:307–316. [PubMed: 10719887]

Li JYH, Joyner AL. Otx2 and Gbx2 are required for refinement and not induction of midhindbrain gene expression. Development 2001;128:4979–4991. [PubMed: 11748135]

Linda H, Hammarberg H, Piehl F, Khademi M, Olsson T. Expression of MHC class I heavy chain and β2-microglobulin in rat brainstem motoneurons and nigral dopaminergic neurons. J Neuroimmunol 1999;101:76–86. [PubMed: 10580816]

Love PE, Shores EW, Johnson MD, Tremblay ML, Lee EJ, Grinberg A, Huang SP, Singer A, Westphal H. T cell development in mice that lack the zeta chain of the T cell antigen receptor complex. Science 1993;261:918–921. [PubMed: 7688481]

Majewska A, Sur M. Motility of dendritic spines in visual cortex in vivo: Changes during the critical period and effects of visual deprivation. Proc Natl Acad Sci USA 2003;100:16024–16029. [PubMed: 14663137]

Malenka RC, Bear MF. LTP and LTD: an embarrassment of riches. Neuron 2004;30:5–21. [PubMed: 15450156]

McLaughlin T, Torborg CL, Feller MB, O'Leary DD. Retinotopic map refinement requires spontaneous retinal waves during a brief critical period of development. Neuron 2003;40:1147–1160. [PubMed: 14687549]

Mrsic-Flogel TD, Hofer SB, Creutzfeldt C, Cloez-Tayarani I, Changeux JP, Bonhoeffer T, Hubener M. Altered map of visual space in the superior colliculus of mice lacking early retinal waves. J Neurosci 2005;25:6921–6928. [PubMed: 16033902]

Muir-Robinson G, Hwang BJ, Feller MB. Retinogeniculate axons undergo eye-specific segregation in the absence of eye-specific layers. J Neurosci 2002;22:5259–5264. [PubMed: 12097474]

Oray S, Majewska A, Sur M. Dendritic spine dynamics are regulated by monocular deprivation and extracellular matrix degradation. Neuron 2004;44:1021–1030. [PubMed: 15603744]

Parnavelas JG, Globus A, Kaups P. Continuous illumination from birth affects spine density of neurons in the visual cortex of the rat. Exp Neurol 1973;40:742–747. [PubMed: 4723854]

Penn AA, Riquelme PA, Feller MB, Shatz CJ. Competition in retinogeniculate patterning driven by spontaneous activity. Science 1998;279:2108–2112. [PubMed: 9516112]

Pfeiffenberger C, Cutforth T, Woods G, Yamada J, Rentería RC, Copenhagen DR, Flanagan JG, Feldheim DA. Ephrin-As and neural activity are required for eye-specific patterning during retinogeniculate mapping. Nat Neurosci 2005;8:1022–1027. [PubMed: 16025107]

Riccio RV, Matthews MA. Effects of intraocular tetrodotoxin on dendritic spines in the developing rat visual cortex: a Golgi analysis. Brain Res 1985;351:173–182. [PubMed: 3995344]

Rossi FM, Pizzorusso T, Porciatti V, Marubio LM, Maffei L, Changeux JP. Requirement of the nicotinic acetylcholine receptor beta 2 subunit for the anatomical and functional development of the visual system. Proc Natl Acad Sci USA 2001;98:6453–6458. [PubMed: 11344259]

Shatz CJ, Stryker MP. Prenatal tetrodotoxin infusion blocks segregation of retinogeniculate afferents. Science 1988;242:87–89. [PubMed: 3175636]

Sholl DA. Dendritic organization in the neurons of the visual and motor cortices of the cat. J Anatomy 1953;87:387–406.

Stevens B, Allen NJ, Vazquez LE, Howell GR, Christopherson KS, Nouri N, Micheva KD, Mehalow AK, Huberman AD, Stafford B, Sher A, Litke AM, Lambris JD, Smith SJ, John SW, Barres BA. The classical complement cascade mediates CNS synapse elimination. Cell 2007;131:1164–1178. [PubMed: 18083105]

Stockton RA, Slaughter MM. B-wave of the electroretinogram. A reflection of ON bipolar cell activity. J Gen Physiol 1989;93:101–122. [PubMed: 2915211]

Stryker MP, Harris WA. Binocular impulse blockade prevents the formation of ocular dominance columns in cat visual cortex. J Neurosci 1986;6:2117–2133. [PubMed: 3746403]

Sun W, Li N, He S. Large-scale morphological survey of mouse retinal ganglion cells. J Comp Neurol 2002;451:115–126. [PubMed: 12209831]

Syken J, Shatz CJ. Expression of T cell receptor β locus in central nervous system neurons. PNAS 2003;100:13048–13053. [PubMed: 14569018]

Syken J, GrandPre T, Kanold PO, Shatz C. PirB restricts ocular-dominance plasticity in visual cortex. Science 2006;313:1795–1800. [PubMed: 16917027]

Taha SA, Stryker MP. Molecular substrates of plasticity in the developing visual cortex. Prog Brain Res 2005;147:103–14. [PubMed: 15581700]

Tian N, Copenhagen DR. Visual Stimulation is required for refinement of ON and OFF pathway in postnatal retina. Neuron 2003;39:85–96. [PubMed: 12848934]

Torborg CL, Meller MB. Unbiased analysis of bulk axonal segregation patterns. J Neurosci Methods 2004;135:17–26. [PubMed: 15020085]

Torborg CL, Hansen KA, Feller MB. High frequency, synchronized bursting drives eye-specific segregation of retinogeniculate projections. Nat Neurosci 2005;8:72–78. [PubMed: 15608630]

Wachtmeister L. Oscillatory potentials in the retina: what do they reveal. Prog Retin Eye Res 1998;17:485–521. [PubMed: 9777648]

Vistamehr S, Tian N. Light deprivation suppresses the light response of inner retina in both young and adult mouse. Vis Neurosci 2004;21:23–37. [PubMed: 15137579]

Wallace W, Bear MF. A morphological correlate of synaptic scaling in visual cortex. J Neurosci 2004;24:6928–6938. [PubMed: 15295028]

Wong RO. Differential growth and remodelling of ganglion cell dendrites in the postnatal rabbit retina. J Comp Neurol 1990;294:109–132. [PubMed: 2324327]

Wong RO. Retinal waves and visual system development. Annu Rev Neurosci 1999;22:29–47. [PubMed: 10202531]

Wong WT, Faulkner-Jones BE, Sanes JR, Wong RO. Rapid dendritic remodeling in the developing retina: dependence on neurotransmission and reciprocal regulation by Rac and Rho. J Neurosci 2000;20:5024–5036. [PubMed: 10864960]

Wong RO, Ghosh A. Activity-dependent regulation of dendritic growth and patterning. Nat Rev Neurosci 2002;3:803–812. [PubMed: 12360324]

Wong RO, Meister M, Shatz CJ. Transient period of correlated bursting activity during development of the mammalian retina. Neuron 1993;11:923–938. [PubMed: 8240814]

Xu HP, Tian N. Retinal ganglion cell dendrites undergo a visual activity-dependent redistribution after eye-opening. J Comp Neurol 2007;503:244–259. [PubMed: 17492624]

Yamasaki EN, Ramoa AS. Dendritic remodeling of retinal ganglion cells during development of the rat. J Comp Neurol 1993;329:277–289. [PubMed: 8454733]

Ziv Y, Ron N, Butovsky O, Landa G, Sudai E, Greenberg N, Cohen H, Kipnis J, Schwartz M. Immune cells contribute to the maintenance of neurogenesis and spatial leaning abilities in adulthood. Nature Neurosci 2006;9:268–275. [PubMed: 16415867]

Zhou ZJ. The function of the cholinergic system in the developing mammalian retina. Progress in Brain Research 2001;131:599–613. [PubMed: 11420974]

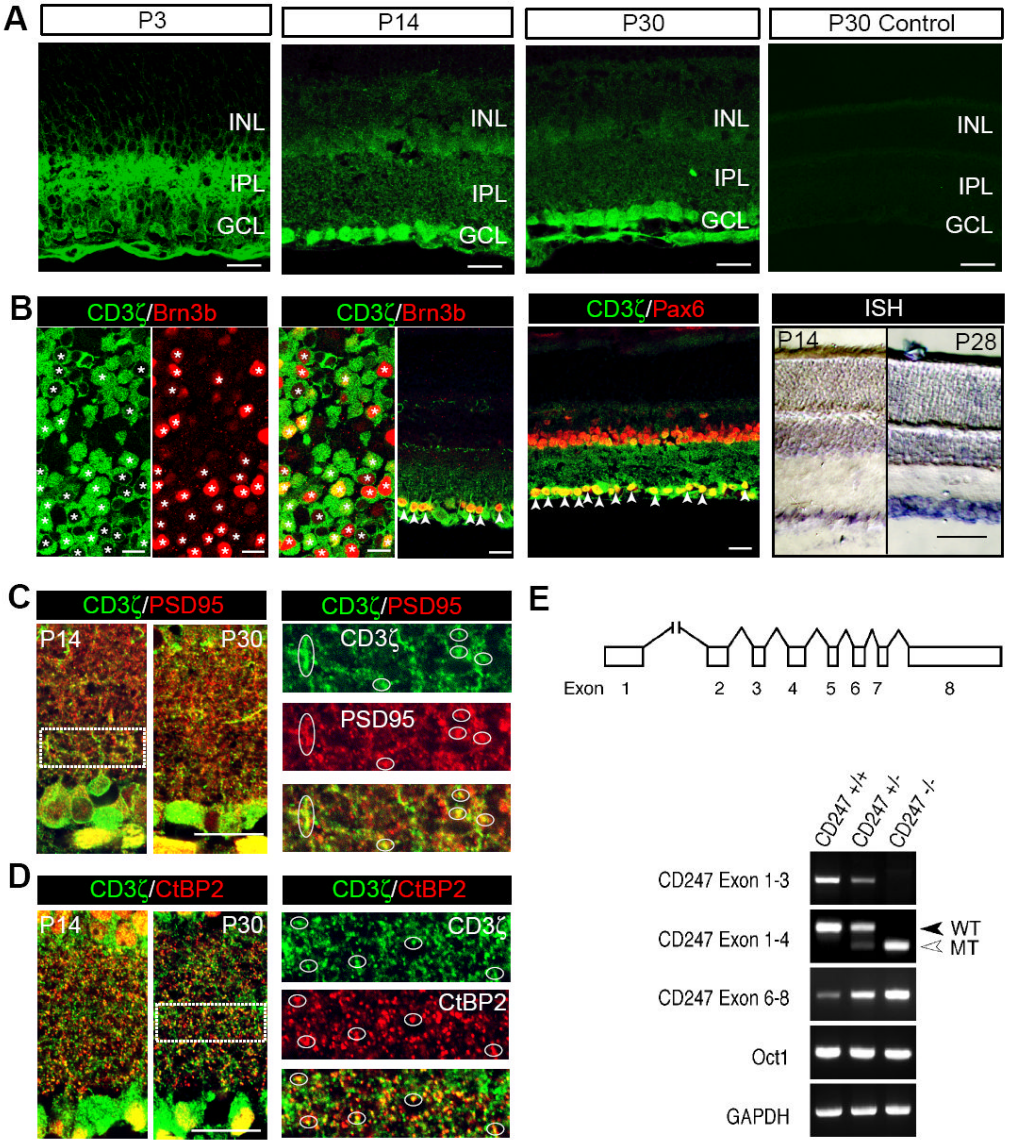

Fig 1. CD3ζ is expressed by RGCs and displaced ACs in mouse retina

(**A**) Anti-CD3ζ antibody labeling shows that CD3ζ is expressed in the inner retina (both IPL and GCL) at P3, P14 and P30. A negative control without primary antibody (P30 Control) shows no labeling. (**B**) Colabeling of CD3ζ with an RGC specific marker, Brn3b, and a pan-AC marker, Pax6, in a flat-mount retina and retinal cross sections from P30 WT mice. CD3ζ is expressed in many, if not all, RGCs (please note that CD3ζ is located in the cytosol while Brn3b is located in the nucleus). CD3ζ is also coexpressed with Pax6 in the GCL, but not the INL. *In situ* hybridization confirms that CD3ζ mRNA is expressed in the GCL in P14 and P28 retinas. (**C**) CD3ζ expression is closely juxtaposed with a postsynaptic marker, PSD95, in both P14 and P30 retinas. Right panels represent the enlarged areas of IPL indicated by the dash-line box in the left panel (P14) and show the overlapping puncta labeled with CD3ζ and PSD95. (**D**) CD3ζ expression is also closely associated with a presynaptic marker, CtBP2, in both P14 and P30 retinas. Right panels represent the enlarged areas of IPL indicated by the dash-line box in the left panel (P30) and show the overlapping puncta labeled with CD3ζ and CtBP2. (**E**) RT-PCR confirmed the expression of CD3ζ

mRNA in WT retina and a truncated mRNA in CD3ζ-/- retina at P30. Top panel: the exon-intron organization of mouse *CD247* genomic locus. Exons are indicated by boxes and introns by lines. Exon 1 is located more than 20 kb upstream of Exon 2. Exon 2 is deleted, and Exon 4 carries a neomycin phosphotransferase (*neo*) gene insertion in the *CD247* mutant allele. Lower panel: total RNA was extracted from the mice indicated and subjected to RT-PCR. *Oct1*, which encodes a ubiquitously expressed nuclear transcription factor, is partially overlapped with and transcribed in an anti-sense orientation relative to *CD247*. GAPDH was used as the internal control. WT, wild type. MT, mutant. Scale bars for 1C and 1D, 100 μm. Scale bars for all other panels of the figure, 20 μm. GCL, ganglion cell layer. INL, inner nuclear layer. IPL, inner plexiform layer.

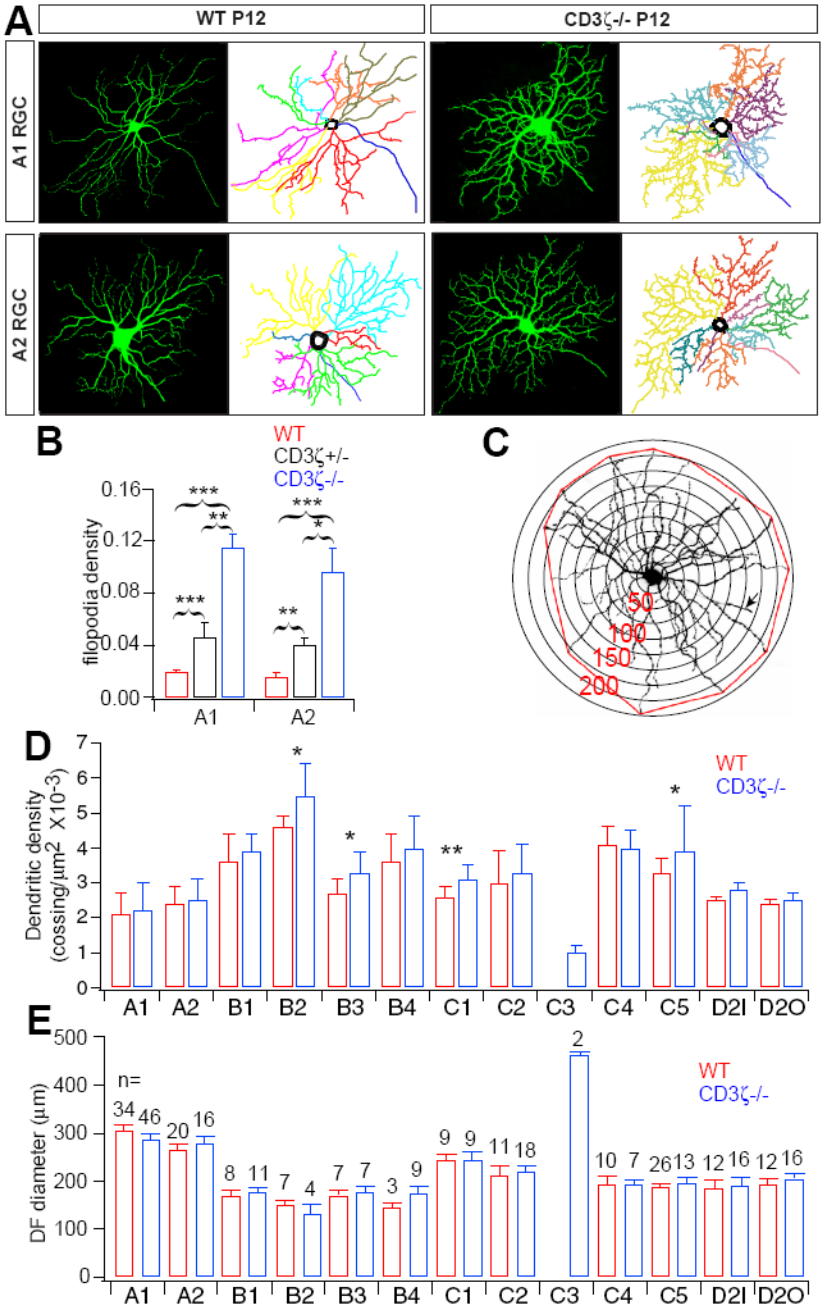

Fig 2. RGCs in immature CD3ζ-/- mice have a higher density of dendritic protrusions

(**A**) Representative images and dendritic reconstructions of A1 and A2 RGCs in P12 WT and CD3ζ-/- mice. (**B**) The average density of dendritic protrusions of A1 and A2 RGCs is abnormally large in CD3ζ-/- mice at P12. (**C**) Sholl analysis was used to examine RGC dendritic density and the dendritic field (DF). (**D**) Average dendritic densities of 12 RGC morphological subtypes at P12. Several morphological subtypes have greater dendritic density in CD3ζ-/- than in WT mice. (**E**) Average DF diameters of 12 morphological subtypes of RGCs were not different in CD3ζ-/- than in WT mice. The number on each bar indicates the number of RGCs in each subgroup. Error bars indicate SEM and * indicates

$0.01 < p < 0.05$. ** indicates $p < 0.01$. *** indicates $p < 0.001$ for this and all following figures. See also Fig S1.

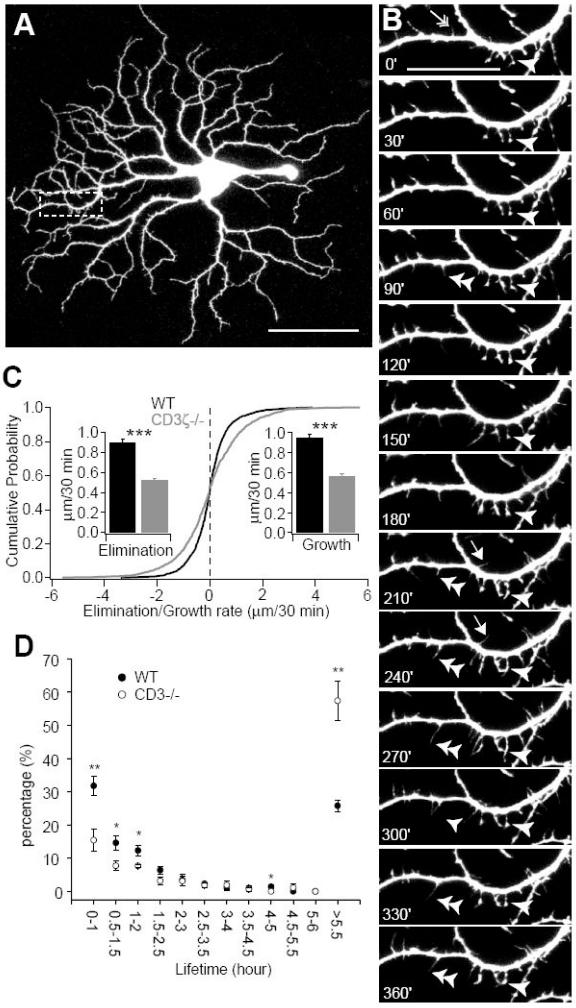

Fig 3. RGC dendritic motility is reduced in CD3ζ-/-mice

RGC dendritic motility was examined using time-lapse confocal imaging on retinas of YFP+ and YFP+/CD3ζ-/- mice at P13-14. (**A**) Representative image of an YFP+ RGC of a WT mouse. Scale bar, 60 μm. (**B**) Representative time-lapse images of a segment of the dendrite from the RGC shown in A (indicated by the dash-line box) taken at 30 minute intervals. Arrow: transient filopodia. Arrowhead: static filopodia. Double arrowhead: new filopodia. Double-headed arrow: filopodia lost over the recording period. Scale bar, 20 μm. (**C**) Cumulative distribution of A1 RGC dendritic kinetics from WT and CD3ζ-/- retinas. Filopodia extension (growth) or retraction (elimination) was determined by the difference of the length of the filopodia recorded at two succeeding time points. Insets, average speed of filopodia elimination and growth. (**D**) Average lifetime of RGC filopodia in WT mice was significantly shorter than CD3ζ-/- mice. Filopodia that existed at the beginning and disappeared before the end of the recording period and filopodia that emerged during the recording period and persisted until the end of the recording were discarded since the lifetime of these filopodia could not be determined. See also movie S1.

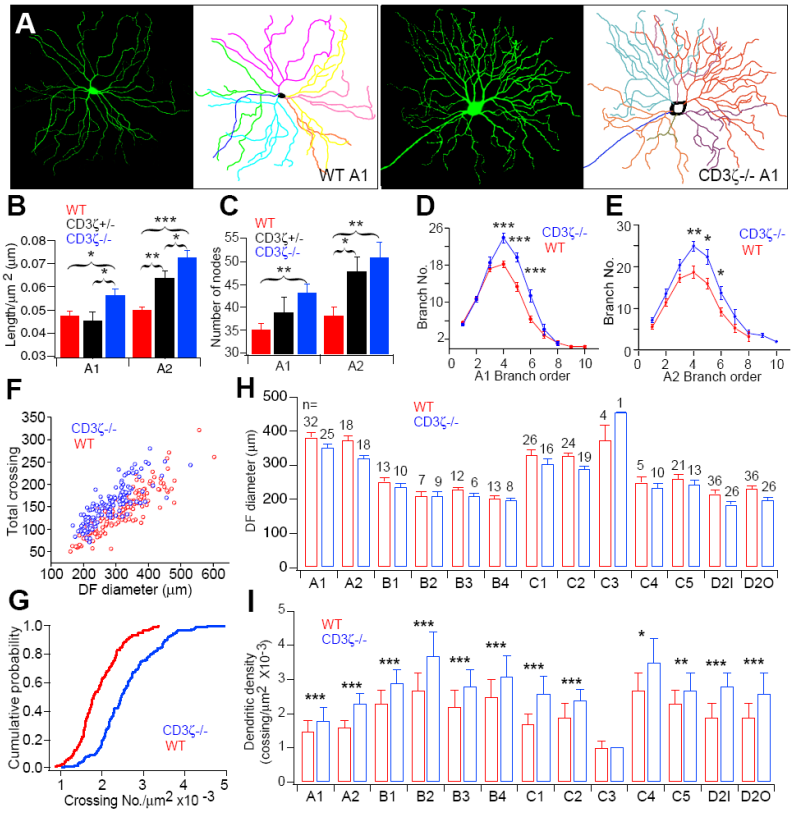

Fig 4. RGC dendritic density increased in mature CD3ζ-/- mice

(**A**) Representative images and tracing results of A1 RGCs from P33 WT and CD3ζ-/- mice. (**B**) Normalized total dendritic length of A1 and A2 RGCs from WT, CD3ζ+/- and CD3ζ-/- mice. (**C**) Total branch number of A1 and A2 RGCs from WT, CD3ζ+/- and CD3ζ-/- mice. (**D**) Branch numbers of A1 RGCs plotted as a function of the branch order of WT and CD3ζ-/- mice. (**E**) Branch numbers of A2 RGCs plotted as a function of the branch order of WT and CD3ζ-/- mice. (**F**) Dendritic density, shown as a function of DF diameter, is higher in P33 CD3ζ-/- than in WT mice. (**G**) Dendritic density, shown as a cumulative distribution, is higher in P33 CD3ζ-/- than in WT mice ($p < 0.0001$, K-S test). Average DF diameters (**H**) and RGC dendritic densities (**I**) broken down into 12 morphological subtypes in WT and CD3ζ-/- mice. See also Fig S2.

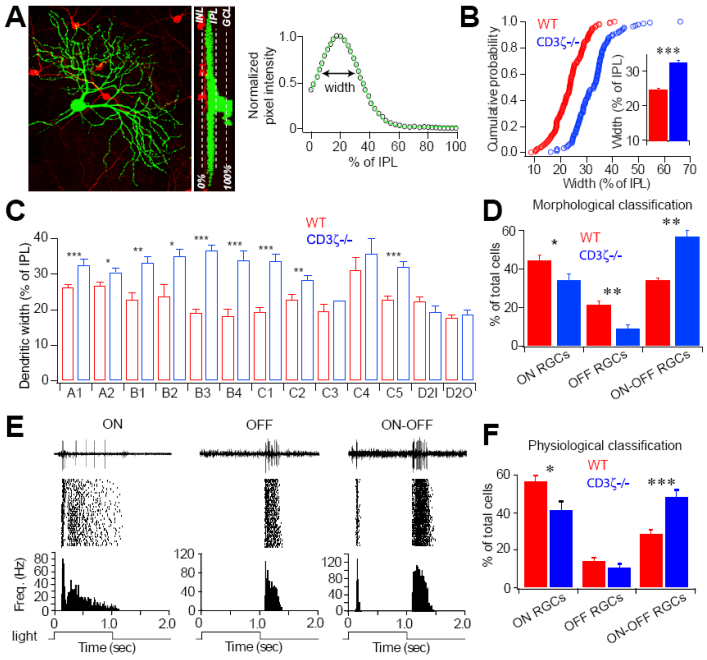

Fig 5. Dendritic stratification and segregation of ON and OFF synaptic inputs onto RGCs are disturbed in P33 CD3ζ-/- mice

The segregation of ON and OFF synaptic pathways was determined morphologically and functionally by examining RGC dendritic ramification in the IPL and light responsiveness in P30-33 mice. (**A**) RGCs were divided into ON, OFF, and ON-OFF classes based on their dendritic distribution patterns in the IPL. This example is an ON RGC with dendrites confined to the ON sublamina. Left panel shows a stacked image, middle panel shows a 90° rotated view and the right panel shows the dendritic stratification for this RGC. (**B**) Cumulative distributions of the dendritic width of RGCs with a single dendritic plexus in WT and CD3ζ-/- mice at P33. Inset: Average dendritic width for these RGCs. (**C**) Dendritic width for each RGC morphological subtype. The dendritic width of 9 out of 12 subtypes increased in CD3ζ-/- compared to WT mice. (**D**) Percentages of the three groups of RGCs based on the morphological classification of their dendritic distribution within exclusively ON, exclusively OFF, or ON and OFF sublamina of the IPL. (**E**) Representative 2-second recordings of light evoked action potentials (top), raster plot of 30 responses (middle) and frequency histogram (bottom) of an ON (left), an OFF (middle), and an ON-OFF (right) cell. The bottom square waves indicate 1-second light stimuli. (**F**) Relative percentages of functionally identified ON, OFF and ON-OFF RGCs of WT and CD3ζ-/- mice at P30.

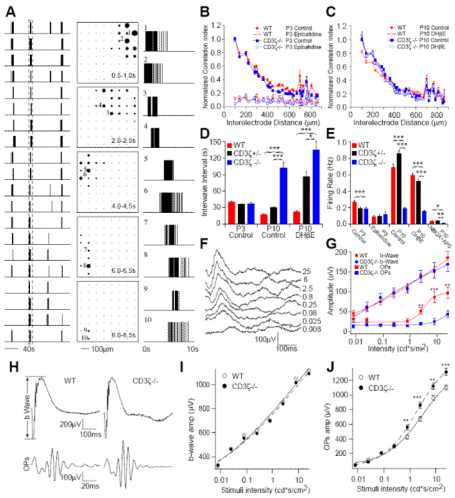

Fig 6. RGC synaptic activity is normal in CD3ζ-/- mice in the first week after birth, but abnormal in the second week

Spontaneous retinal waves, mediated by nAChRs during the first postnatal week and GluRs during the second postnatal week, were recorded from WT, CD3ζ+/- and CD3ζ-/- mice using a MEA system. Light evoked inner and outer retinal responses were measured using electroretinogram (ERG) recordings at P14 and P30 in WT and CD3ζ-/- mice. **(A)** Example of retinal waves recorded from a P10 WT retina. Left column: Spike trains from twenty neurons. Center column: Diagrams of the array show the propagation of a wave from the top right to the bottom left. Each frame shows the firing rate averaged over 0.5 sec. Each black circle represents one cell, with the radius of the circle proportional to its firing rate. Right column: Spike trains of ten neurons selected from the time window shown in the left column. The position of each neuron is represented with the number in the center column. **(B)** Normalized correlation index, taken from the MEA recordings in P3 WT, CD3ζ+/- and CD3ζ-/- mice. Retinal waves in WT, CD3ζ+/- and CD3ζ-/- mice are blocked by bath application of 10 nM Epibatidine, a nAChR agonist. **(C)** Normalized correlation index in P10 WT, CD3ζ+/- and CD3ζ-/- mice. Pharmacological manipulation of nAChRs had no effect on retinal waves in the second week. **(D)** Average interwave interval in WT, CD3ζ+/- and CD3ζ-/- mice at P3 and P10, showing that waves are much less frequent in CD3ζ-/- in the second week. **(E)** Average firing rate of WT, CD3ζ+/- and CD3ζ-/- mice at P3 and P10. (**F**) Representative ERGs recorded from a P14 WT mouse evoked by eight different light intensities. (**G**) The average amplitudes of ERG b-waves and OPs of CD3ζ-/- and WT mice recorded at P14. (**H**) Representative ERG and OP waveforms from P30 WT and CD3ζ-/- mice. (**I**) Average amplitude of ERG b-waves. (**J**) Average amplitude of ERG OPs are significantly bigger in CD3ζ-/- mice.

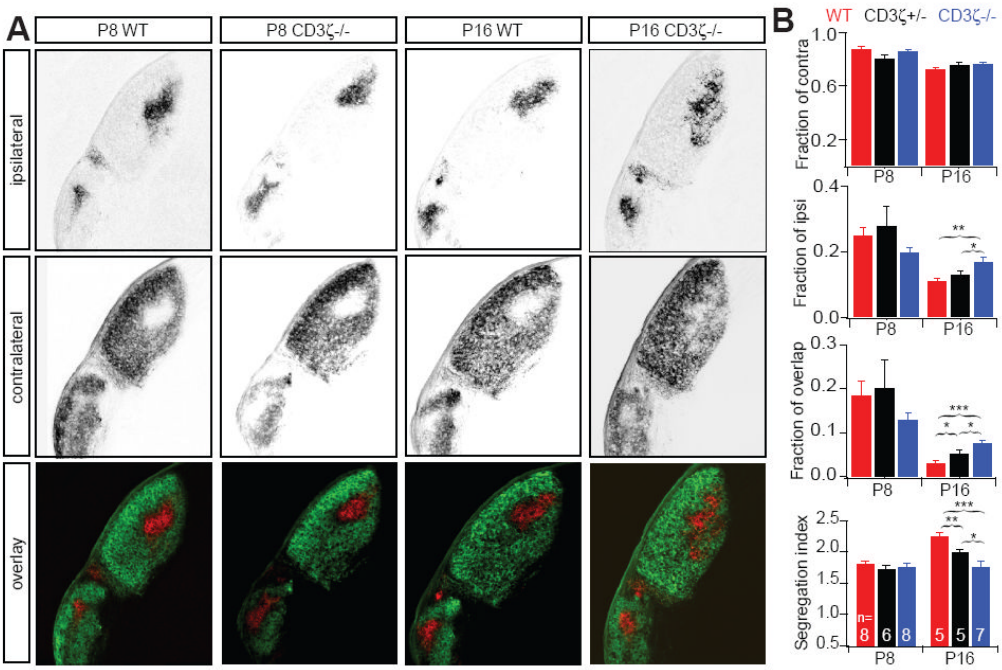

Fig 7. Eye-specific segregation in CD3ζ-/- mice is normal at P8 but disrupted at P16

(**A**) Representative fluorescent images of ipsilateral (upper) and contralateral (middle) RGC axon projections to the dLGN of WT and CD3ζ-/- mice at P8 and P16. The lower row shows an overlay of the two projections, with ipsilateral in red and contralateral in green. **(B)** Summary quantification of RGC axon projections of WT, CD3ζ+/- and CD3ζ-/- mice at P8 and P16, show the fraction of contralateral, ipsilateral and overlap projections in the dLGN and the Segregation Index (mean variance). Axons are similarly segregated at P8, but axons, especially for ipsilateral projections, occupy larger area of dLGN in CD3ζ+/- than in WT mice at P16 and overlapped with projections from the contralateral eye. See also Fig S3.

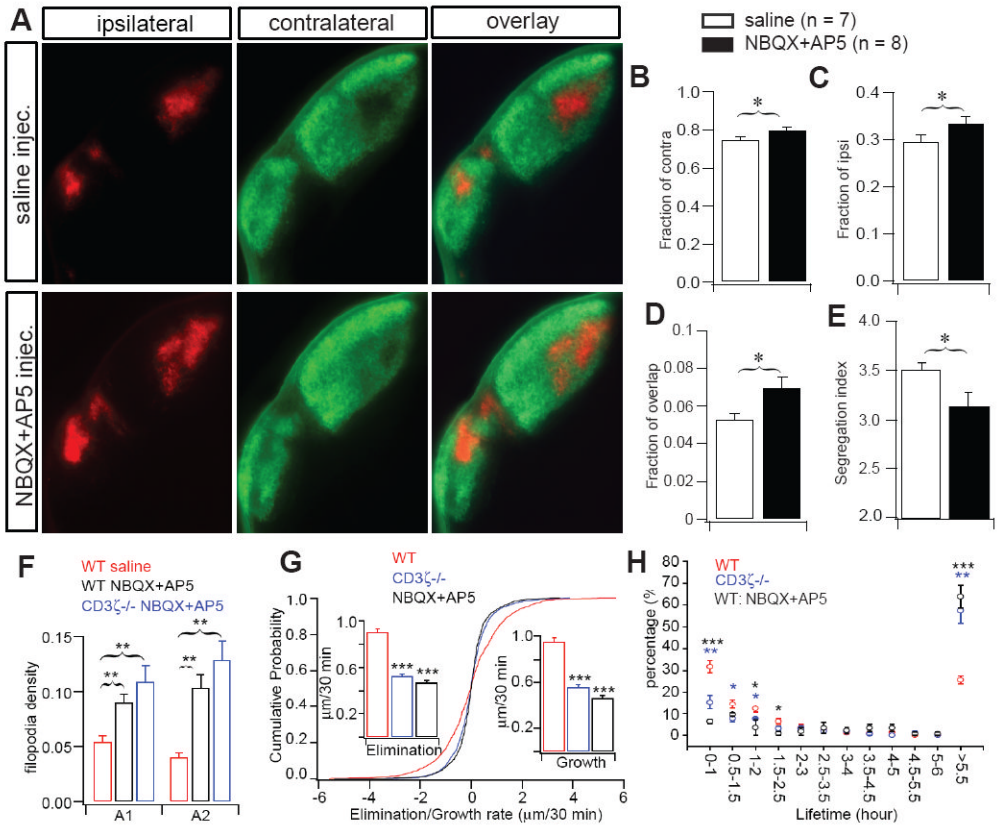

Fig 8. GluR-mediated synaptic activity regulates the maturation of RGC axonal projections and dendritic structure

Blockade of glutamatergic synaptic transmission in WT retina disrupts eye specific segregation of RGC axons to the dLGN, mimicking the effects of genetic deletion of CD3ζ. (**A**) Representative fluorescent images of ipsilateral (red) and contralateral (green) RGC axon projections to the dLGN of P14 WT mice that received daily binocular injections of either saline (top) or NBQX+AP5 (bottom) from P7-P12. Quantification of the fraction of contralateral (**B**), ipsilateral (**C**) and overlap (**D**) projections in the dLGN and the Segregation Index (**E**) in WT mice at P14 with or without NBQX+AP5 treatment. Intraocular treatment with glutamate receptor antagonists disrupted e eye-specific segregation compared with saline treated controls. (**F-H**) Blocking glutamatergic neurotransmission in WT retina fully recapitulates the reduced RGC dendritic pruning observed in CD3ζ-/- mice. (**F**) The average density of dendritic protrusions is higher in A1 and A2 RGCs in P12 WT mice that have had chronic intraocular application of GluR antagonists (NBQX and AP5) from P7-P11. Application of the GluR antagonists to CD3ζ-/- mice has no additional effect. (**G**) Cumulative distribution of A1 RGC dendritic kinetics from WT retinas in control solution, WT retinas in the presence of 10 μM NBQX + 100 μM AP5, and CD3ζ-/- retinas in control solution. Bath application of NBQX + AP5 reduced the dynamics of filopodia extension and retraction to the same level as that observed in CD3ζ-/- retinas. (**H**) Blockade of glutamate neurotransmission increased the average lifetime of RGC filopodia in WT mice, mimicking the effects induced by genetic deletion of CD3ζ. Please note that the data shown in this figure was collected using a regular epifluorescent microscope while the data shown in figure 7 was collected using a laser confocal microscope. Therefore, the actual values of the result, especially the ipsilateral staining, are different in these two figures.